Katarzyna Borowiec
Department of Nuclear, Plasma and Radiological Engineering,
University of Illinois at Urbana-Champaign,
Urbana, IL 61801
e-mail: kb6@illinois.edu

Aaron Wysocki
Reactor and Nuclear Systems Division,
Oak Ridge National Laboratory,
Oak Ridge, TN 37830
e-mail: wysockiaj@ornl.gov

Samuel Shaner
Yellowstone Energy,
Oak Ridge, TN 37830
e-mail: sam@yellowstone.energy

Michael S. Greenwood
Reactor and Nuclear Systems Division,
Oak Ridge National Laboratory,
Oak Ridge, TN 37830
e-mail: greenwoodms@ornl.gov

Matthew Ellis
Yellowstone Energy,
Oak Ridge, TN 37830
e-mail: matt@yellowstone.energy

Increasing Revenue of Nuclear Power Plants With Thermal Storage

Introducing large amounts of electricity produced from variable renewable energy sources such as wind and solar decreases wholesale electricity price while increasing the volatility of the market. These conditions drive the need for peak-load power generation, while regulation requirements fuel the push for flexible power generation. The increase of variable renewable energy in the market share, along with falling natural gas prices, makes nuclear power plants less competitive. Thermal storage is being considered to increase the nuclear power plant revenue. Thermal storage increases the flexibility of the nuclear plant system without sacrificing its efficiency. There are multiple opportunities to increase the nuclear power plant revenue, including increased capacity payments, arbitrage, and ancillary services. An economic analysis was performed to investigate the revenue increase of the system with thermal storage. The investment cost was assessed, and net present value was evaluated for the considered scenarios. Two system designs were considered in the analysis: a thermal storage system using the existing power conversion infrastructure and an integrated design with thermal storage fully incorporated into the reactor system design. The preliminary analysis showed that introducing a thermal storage system is profitable for some scenarios considered. Profitability depends significantly on the storage size, output flexibility, share of variable renewable energy, and market characteristics. [DOI: 10.1115/1.4044800]

1 Introduction

The pursuit of clean energy has increased the share of variable renewable energy (VRE), affecting the wholesale electricity prices. Those changes can influence the operation and profitability of the nuclear power plant (NPP) [1,2]. Figure 1 illustrates the difference between wholesale energy prices for market with low VRE and high VRE shares. A higher share of VRE in the energy market changes the price profile significantly: the price of the wholesale electricity decreases, and the market volatility increases. A higher number of low-priced hours are also observed [3].

An increase in VRE drives the cost of electricity down due to its low marginal cost. However, VRE resources are characterized by uncontrollable availability that does not correspond to the peak-power demand. This drives the price up when the demand is high, and the supply of VRE goes down. The increased share of VRE has a significant impact on the ancillary services market. The electricity production is not easily predicted, which introduces uncertainty in the market and drives the need for higher reserve, which in turn increases the cost of ancillary services [3]. These conditions decrease the need for base load power generation and favor the peak power generators with flexible operation capabilities.

When these conditions are combined with decreased natural gas prices, NPPs struggle to remain competitive in the energy market. Two main ideas are being considered to increase the NPP profitability: energy storage [1] and cogeneration [4–6]. Due to the high cost of batteries, thermal storage (TS) is currently the most promising option. Cogeneration plans include hydrogen production [7], desalination [8], and district heating coupling [9].

Different types of TSs are possible, including steam accumulators, a sensible heat fluid system [10,11], a cryogenic air system [12], packed bed thermal energy storage [13–15], hot rock storage [16], and geothermal heat storage [1,17]. This study investigated latent heat storage, a mature technology that is already widely used for solar energy storage systems.

Multiple studies have shown the possibility of TS coupling [18–21]. This analysis emphasizes the economic benefit of the TS system. Introducing TS to the power plant can bring additional revenue through the following:

1. **Arbitrage**: Additional revenue can be realized by taking advantage of energy prices, selling more electricity during higher demand (higher price), and charging the storage system when the demand goes down (lower price).
2. **Capacity**: TS increases the capacity of the system and hence the capacity payments.
3. **Ancillary services**: Grid stability is becoming an issue as the market share of VRE increases. Introducing flexibility to power generation provides the opportunity to increase the revenue for ancillary services.

The analysis was conducted using a price forecast for 2030 [3]. Different geographical regions and various scenarios of the VRE market share were considered. The summary of scenarios is presented in Table 1. Four energy markets were modeled: Southwest Power Pool (SPP), New York Independent System Operator (NYISO), California Independent System Operator (CAISO), and Electric Reliability Council of Texas (ERCOT). For a detailed description of energy markets, see Ref. [3]. Four scenarios were considered for each operator: (1) low VRE, in which the level of VRE was assumed to remain at the 2016 level, (2) balanced case, which considered equal shares of wind and solar energy at the 20% level, (3) high wind scenario, which assumed 30%

Contributed by the Advanced Energy Systems Division of ASME for publication in the Journal of Energy Resources Technology. Manuscript received September 12, 2018; final manuscript received September 4, 2019; published online September 10, 2019. Assoc. Editor: Ashwani K. Gupta.

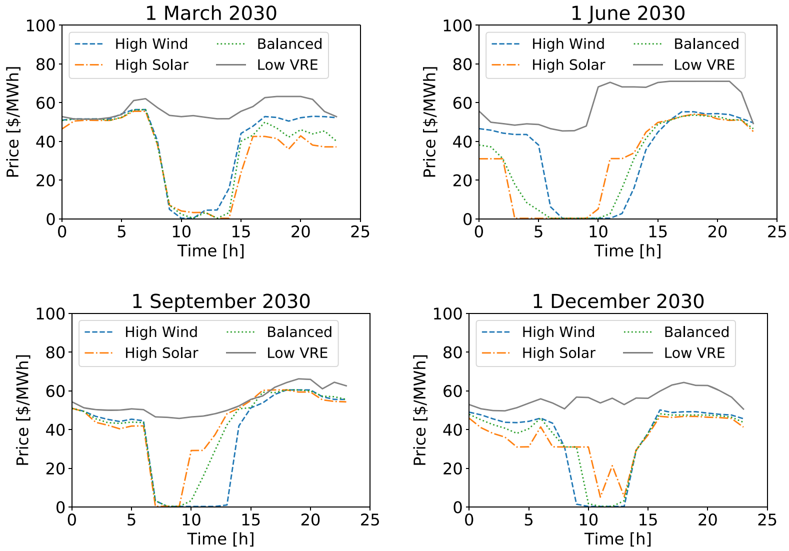

Fig. 1 Wholesale energy prices with different shares of VRE, California independent system operator, predicted prices for 2030 [3]

Table 1 Summary of scenarios and assumptions for the price data [3]

Share of VRE	
Low VRE	Level from 2016
Balanced VRE	20% wind and 20% solar
High wind	30% wind and 10% solar
High solar	10% wind and 30% solar
Assumptions	
ConCap	Consistent capacity balancing
LimCap	Limited capacity balancing

Table 2 Capacity prices for 2030 [3]

Price [$/kW-year]	CAISO	NYISO	ERCOT	SPP
Low VRE	$72.20	$18.42	$54.20	$54.47
LimCap balanced	$58.59	$50.40	$62.57	$76.92
LimCap high wind	$59.25	$46.88	$65.31	$76.71
LimCap high solar	$59.02	$54.2	$71.89	$76.48
ConCap balanced	$56.39	$51.17	$55.24	$76.23
ConCap high wind	$55.76	$51.82	$71.22	$74.27
ConCap high solar	$56.31	$55.21	$70.56	$76.35

wind with at least 10% solar energy, and (4) high solar case, in which solar energy was at the level of 30% with at least 10% wind.

The last assumption considered retirement of the non-VRE portfolio. Two cases were considered: (1) consistent capacity balancing (ConCap), in which the generator capacity was eliminated if the O&M cost could not be recovered due to a high share of the VRE, and (2) limited capacity balancing (LimCap), in which the VRE portfolio was assumed to not affect the non-VRE portfolio. The latter case led to significant overcapacity in some cases.

The analysis was conducted using two models: a capacity expansion model (Gen-X) for the determination of the non-VRE generation shares and a market simulation model (UPLAN) to optimize the hourly energy and ancillary services prices. For detailed descriptions of assumptions made and the models used, see Ref. [3].

The models were used to determine the wholesale energy prices, ancillary services, and capacity payments. The capacity payments for each scenario are presented in Table 2. Examples of the ancillary prices and wholesale energy prices are presented in the box plots in Figs. 2 and 3, respectively. In these figures, rectangle represents first and third quartile and lines represent the 95% confidence intervals around the median.

2 Methods

Different limitations need to be considered for different designs. For the design that uses existing infrastructure (hereafter referred to as the “add-on design”), there are limitations on the rate of diverting the steam to the heat storage system. According to Ref. [1], a TS system may safely divert 20%–25% of the steam when charging the system, and it may increase the peak power output by about 4%–5% by utilizing the existing infrastructure. For the fully integrated design in which all of the elements are designed to operate with a varying power load, variation can be much higher: in this study, the integrated design power was allowed to vary between 50% and 150% of the nominal power. The two TS system coupling methods are presented in Fig. 4. The integrated design places the TS system in the intermediate loop, where all of the coolant goes through the storage tank. The add-on design redirects the part of the steam to the TS system, which is separate from the reactor infrastructure and requires additional heat exchangers.

Determination of the investment’s profitability requires determination of cost and revenue. However, cost and revenue depend on the system design and can be tightly connected. In the case of TS, the bigger the system, the higher the possible revenue increase, and also the higher the cost. Optimization needs to be performed to determine the system size. In addition, to determine the increase of revenue that can be achieved through arbitrage and by providing ancillary services, the system state must be known at every hour of the year.

Investment decisions should be guided by a realistic assessment of investment cost. However, for most systems, there are a few key elements used in determining the cost. Those elements, along with their assessed costs [22,23], include the following:

1. Add-on TS system
    1. **Heat exchanger**: TS requires additional heat exchangers. Assumed cost: 300$/kW$_{th}$ for the steam generator and 10$/kW$_{th}$ for the condenser.

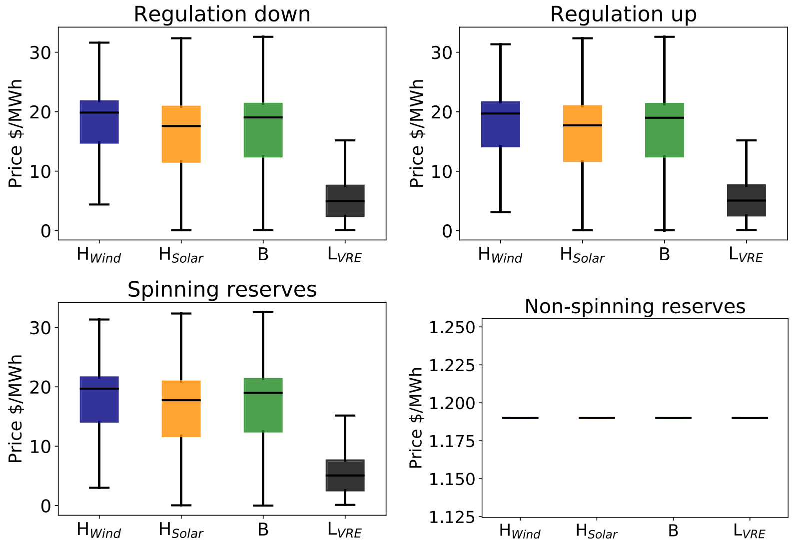

Fig. 2 Ancillary services, CAISO [3]

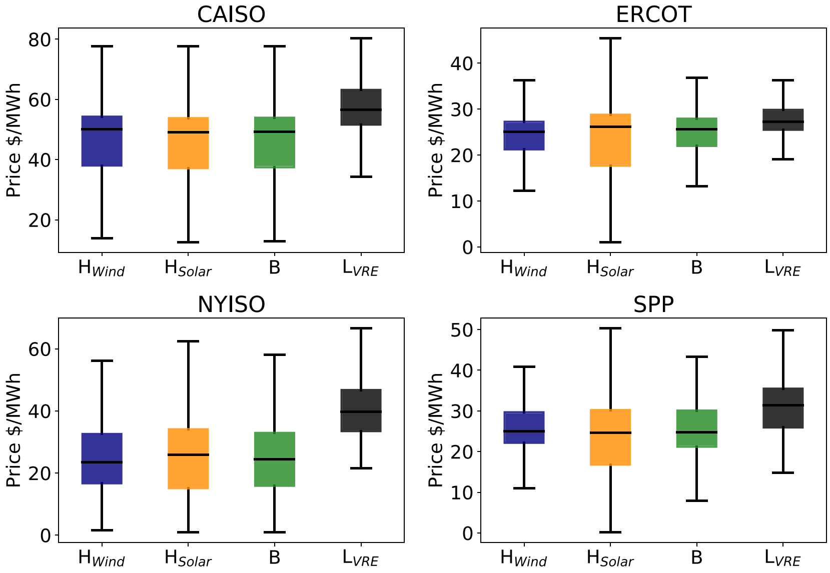

Fig. 3 Wholesale energy prices [3]

   (b) **Storage tank**: The cost of the tank includes the heat transfer fluid, materials, additional space, etc. Assumed cost: 50\$/kWh$_{\text{th}}$. The heat exchange fluid is Therminol® VP1 [24].

(2) Integrated TS system
   (a) **Steam generator**: For the integrated TS system, the capacity of the steam generator is increased to accommodate the power increase. Assumed cost: 300\$/kW$_{\text{th}}$.
   (b) **Turbine**: The system operates at an increased power, so turbine capacity must be increased. Assumed cost: 23 \$/kW$_{\text{th}}$.
   (c) **Condenser and other elements**: Assumed cost: 10 \$/kW$_{\text{th}}$.
   (d) **Storage tank**: The cost of the tank includes the heat transfer fluid, materials, additional space, etc. Assumed cost: 20\$/kWh$_{\text{th}}$. The heat exchange fluid is molten salt.

An optimization tool was created to determine the state of the system at each hour and to optimize the system size. Figure 5 presents the general idea behind the algorithm. For each time step, the state of the system is determined as follows. First, the level of the TS is checked. If the storage system is fully charged (the TS system is empty), then the charging (power raise) option is excluded for this time step. Next, the mean (μ) and standard deviations are evaluated based on the time steps in the range T_{look} away from the current time step. Based on the price for the current time step, the decision is made whether to raise the system's power, lower it, or keep it at the nominal level. The system state also depends on the TS level (F_S); a mechanism is added to favor charging the system if the TS is empty and discharging the system if the TS is full. This mechanism was added to ensure the highest possible utilization factor for the TS. The parameters in the model and the size of the storage are determined through an optimization process by sampling from the space of the possible values and determining the most optimal case based on the net present value (NPV). If the system operates at nominal power, then revenue from ancillary services can be added, constrained by the storage level. Information on whether the utility is called on to provide the ancillary service was not provided; therefore, for the purpose of the simulation, it is assumed that the utility is *not* called on to provide the service, that the plant will clear the capacity auction, and that the ancillary market admits all changes in power of the system.

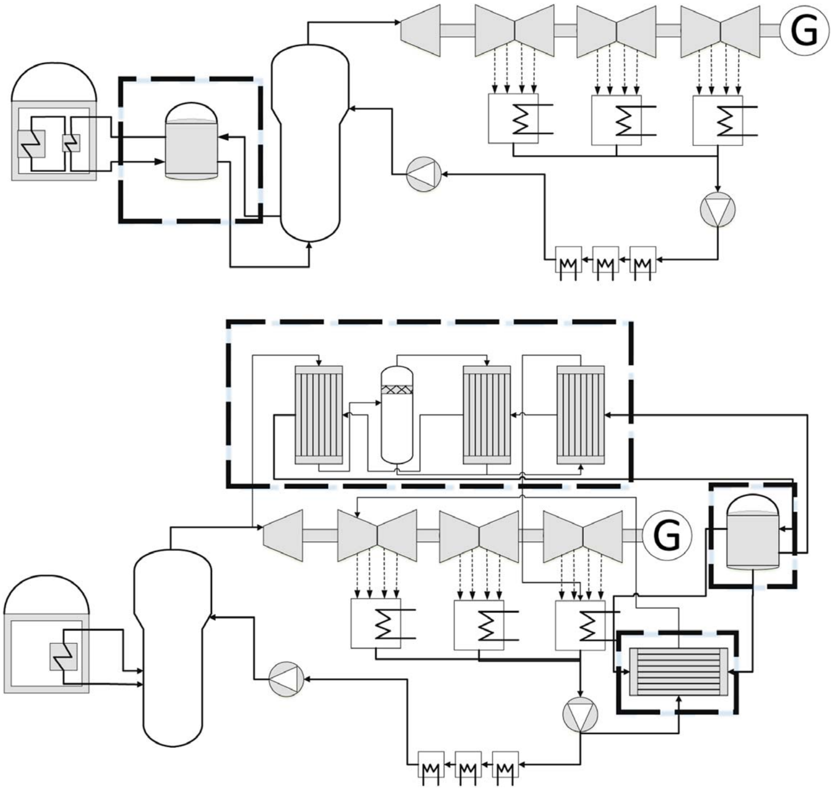

Fig. 4 Schematic representation of the considered designs. Integrated design is on the top, and add-on design is on the bottom.

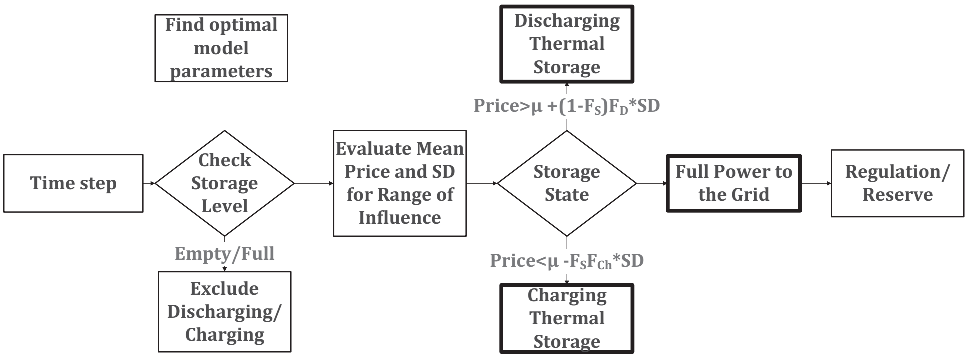

Fig. 5 Optimization tool, working principle. F_{Ch} and F_D are fraction of power output during charging and discharging of the thermal system, respectively.

Different measures can be considered in the investment analysis. In this study, NPV was used as a measure of investment profitability. The NPV is the difference between the present value of cash inflows and the present value of cash outflows over a certain time period; NPV was calculated as follows:

$$\mathrm{NPV} = \sum_{n=1}^{N} \frac{C_n}{(1+DR)^n} - C_0 \qquad (1)$$

where N is a duration of investment, DR is the discount rate, C_0 is the initial investment, and C_n is the additional revenue due to investment for the nth year.

3 Results and Discussion

The optimization tool was used to evaluate the increased revenue for both cases. The NPP was assumed to have a thermal power of 3500 MW and an efficiency of 33%. The NPV of the investment was evaluated for the 20-year period with the discount rate of 5.5%. The increase in revenue was assumed to be constant through the investment period. The results for the add-on design are presented in Table 3 and Fig. 6, and the results for the integrated design are provided in Table 4 and Fig. 7.

The results include the case study with information about energy market, share of VRE, and the capacity balancing type. Moreover, the investment NPV, base revenue (R_B), revenue with TS (R_M), and optimized size of the storage (S_C) are presented. The storage capacity was investigated in increments, depending on the flexibility of the system. The minimum storage level was set to assess the proximity to the break-even point. For the add-on design, 7 of 28 cases were shown to be profitable. For all regions, the least profitable investment was observed for the low VRE scenario. This is due to lower variability of the wholesale energy prices, as well as the lower price of providing ancillary services. All of the cases with NPVs above zero were realized for the CAISO and ERCOT

Table 3 Range base model results for each scenario, add-on design

Set	Case	Cap.	NPV [mln \$]	R_B [mln \$]	R_M [mln \$]	S_C [MWh]
CAISO	LowVRE	–	−21.86	581.67	583.57	700.0
	Balanced	LimCap	1.41	452.71	457.36	700.0
		ConCap	−2.99	447.46	451.86	700.0
	HighWind	LimCap	−7.5	450.63	454.49	700.0
		ConCap	14.94	435.14	441.08	700.0
	HighSolar	LimCap	18.59	443.66	449.72	700.0
		ConCap	-8.07	446.85	450.83	700.0
ERCOT	LowVRE	–	−16.69	331.67	335.05	700.0
	Balanced	LimCap	12.4	256.83	262.16	700.0
		ConCap	18.34	274.57	280.82	700.0
	HighWind	LimCap	−1.44	256.86	260.87	700.0
		ConCap	−3.92	253.57	257.04	700.0
	HighSolar	LimCap	28.82	262.32	268.49	700.0
		ConCap	37.11	280.22	287.16	700.0
NYISO	LowVRE	–	−58.5	412.08	414.03	700.0
	Balanced	LimCap	−25.26	248.82	251.7	700.0
		ConCap	−24.71	248.62	251.5	700.0
	HighWind	LimCap	−29.75	253.03	255.74	700.0
		ConCap	−25.6	252.48	255.26	700.0
	HighSolar	LimCap	−17.66	252.47	255.77	700.0
		ConCap	−17.26	250.18	253.45	700.0
SPP	LowVRE	–	−40.5	317.98	319.35	700.0
	Balanced	LimCap	−6.65	247.86	250.77	700.0
		ConCap	−6.92	248.23	251.16	700.0
	HighWind	LimCap	−8.3	252.39	255.17	700.0
		ConCap	−8.95	254.95	257.82	700.0
	HighSolar	LimCap	−2.12	232.24	235.56	700.0
		ConCap	−2.75	232.2	235.47	700.0

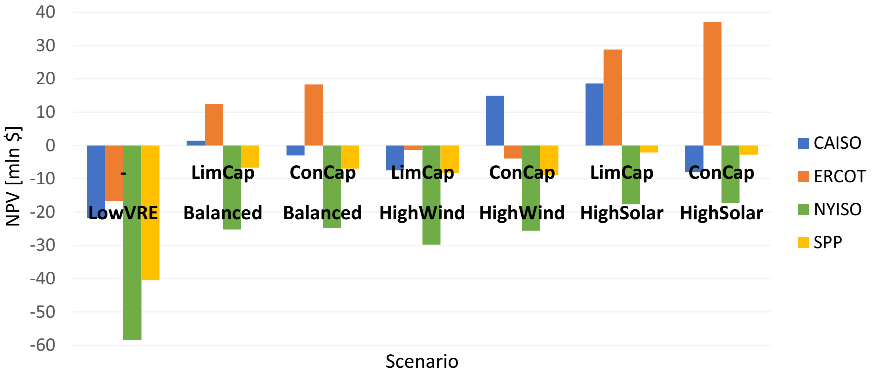

Fig. 6 Range base model NPV results for each scenario, add-on design

regions. No profitable investments were observed for the NYISO and SPP markets.

Differences between the energy markets depend mostly on the periodicity of the energy prices and how they change during the day. For all cases, the minimum possible storage size was found to be optimal due to the high price of the storage tank and the high cost of increasing the tank size. This storage size corresponds to 1 h of charging the TS; since the power can be increased only by 5%, this corresponds to 4 h of increased power. The time of charging the system and power increase was evaluated based on the storage capacity and nominal power. In addition, due to the limitation on the power increase in this design, increasing the size of the TS will have no effect on capacity payments and ancillary services.

The fully integrated case is characterized by a higher increase in revenue due to higher system flexibility. The increase in capacity payments is higher, and the same is true for the arbitrage and ancillary services. As in the case for the add-on design, the low VRE case is the least profitable for each region. The optimal storage size was found to be at the lower limit for most of the cases, as was the case for the add-on design.

However, there are a few cases in which the optimal storage size was significantly higher. This shows the dependence of the system design on the energy market and share of the VRE.

4 Conclusions

This investigation included an economic analysis of the TS concept for increasing the flexibility and the profitability of NPPs. There are numerous sources of increased profit that occur when flexibility in plant operation increases. This analysis used available cost and electricity price data. Capacity payments, arbitrage, and ancillary payments were considered.

The operation of the power plant and the size of the storage system were determined through the use of an optimization tool that assessed the revenue increase for the system. Different

Table 4 Range base model results for each scenario, integrated design

Set	Case	Cap.	NPV (mln $)	R_B (mln $)	R_M (mln $)	S_C (MWh)
CAISO	LowVRE	–	1.78	574.85	590.69	5200.0
	Balanced	LimCap	251.97	447.41	486.09	1700.0
		ConCap	230.28	442.22	480.34	1700.0
	HighWind	LimCap	150.91	445.35	475.2	1700.0
		ConCap	425.4	430.04	484.85	1700.0
	HighSolar	LimCap	467.73	438.47	494.96	1700.0
		ConCap	136.32	441.62	471.92	1700.0
ERCOT	LowVRE	–	47.11	327.78	360.53	6900.0
	Balanced	LimCap	398.09	253.82	302.46	1700.0
		ConCap	406.85	271.35	324.91	1700.0
	HighWind	LimCap	245.57	253.85	288.16	1700.0
		ConCap	241.78	250.6	281.23	1700.0
	HighSolar	LimCap	486.88	259.25	310.0	1700.0
		ConCap	572.87	276.94	344.34	6900.0
NYISO	LowVRE	–	−329.18	407.25	423.25	3500.0
	Balanced	LimCap	−23.26	245.91	266.23	1700.0
		ConCap	−16.32	245.71	266.17	1700.0
	HighWind	LimCap	−49.83	250.06	270.18	1700.0
		ConCap	−19.61	249.53	269.35	1700.0
	HighSolar	LimCap	51.72	249.51	273.94	1700.0
		ConCap	58.32	247.25	271.66	1700.0
SPP	LowVRE	–	−135.1	314.26	322.9	1700.0
	Balanced	LimCap	204.75	244.96	269.23	1700.0
		ConCap	187.54	245.32	268.55	1700.0
	HighWind	LimCap	210.38	249.43	274.29	1700.0
		ConCap	185.52	251.97	276.14	1700.0
	HighSolar	LimCap	242.94	229.52	257.24	1700.0
		ConCap	243.67	229.48	257.33	1700.0

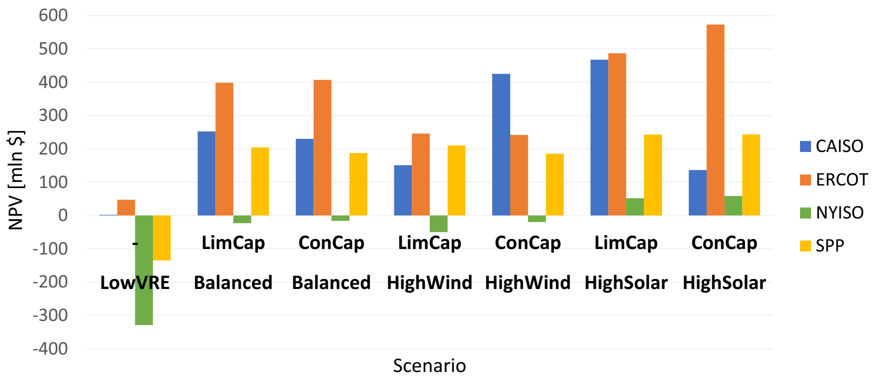

Fig. 7 Range base model NPV results for each scenario, integrated design

scenarios were considered using electricity prices for multiple regions, as well as different shares of VRE. Two TS coupling design types were considered. Depending on the design, profitability of the investment was realized for some or most of the scenarios considered. The operational flexibility allowed in the system is the main parameter governing the revenue. The benefit from the TS system is much more evident for the high VRE scenario, mainly due to the increased variability of the wholesale energy prices and the higher ancillary services price with the increased VRE.

In the analysis, dependence on the market and dependence on market conditions were demonstrated. The profitability of investment and the optimal system size are tightly connected to the energy market, including the share of energy resources, the installed capacity, and the types of markets present in the region. The materials and installation costs of the TS system, as well as the increased maintenance cost, should also be considered.

The analysis showed that TS is a promising technology that can increase the flexibility of NPP operation and increase the revenue through arbitrage, capacity payments, and ancillary services.

Acknowledgment

This manuscript has been authored by UT-Battelle, LLC, under contract DE-AC05-00OR22725 with the US Department of Energy (DOE). The US government retains and the publisher, by accepting the article for publication, acknowledges that the US government retains a nonexclusive, paid-up, irrevocable, worldwide license to publish or reproduce the published form of this manuscript, or allow others to do so, for US government purposes. DOE will provide public access to these results of federally sponsored research in accordance with the DOE Public Access Plan (http://energy.gov/downloads/doepublic-access-plan).

This research was supported in part by an appointment to the NESLS Program at Oak Ridge National Laboratory (Funder ID: 10.13039/100006228).

References

[1] Forsberg, C., Brick, S., and Haratyk, G., 2018, "Coupling Heat Storage to Nuclear Reactors for Variable Electricity Output With Baseload Reactor Operation," Electr. J., **31**(3), pp. 23–31.

[2] Misenheimer, C. T., and Terry, S. D., 2017, "Modeling Hybrid Nuclear Systems With Chilled-Water Storage," ASME J. Energy Res. Technol., **139**(1), p. 012002.

[3] Seel, J., Mills, A. D., and Wiser, R. H., 2018, "Impacts of High Variable Renewable Energy Futures on Wholesale Electricity Prices, and on Electric-Sector Decision Making," Technical Report No. 05/2018. Lawrence Berkeley National Laboratory.

[4] Orhan, M., Dincer, I., and Naterer, G., 2008, "Cost Analysis of a Thermochemical Cu–Cl Pilot Plant for Nuclear-Based Hydrogen Production," Int. J. Hydrogen Energy, **33**(21), pp. 6006–6020.

[5] Ingersoll, D. T., Houghton, Z. J., Bromm, R., and Desportes, C., 2014, "Nuscale Small Modular Reactor for Co-generation of Electricity and Water," Desalination, **340**(1), pp. 84–93.

[6] Jedrzejewski, J., and Hanuszkiewicz-Drapala, M., 2018, "Analyses of the Efficiency of a High-Temperature Gas-Cooled Nuclear Reactor Cogeneration System Generating Heat for the Sulfur–Iodine Cycle," ASME J. Energy Res. Technol., **140**(11), p. 112001.

[7] Jianu, O., Naterer, G., and Rosen, M., 2016, "19–Hydrogen Cogeneration With Generation IV Nuclear Power Plants," *Handbook of Generation IV Nuclear Reactors* (Woodhead Publishing Series in Energy), I. L. Pioro, ed., Woodhead Publishing, Sawston, Cambridge, pp. 637–659.

[8] Asiedu-Boateng, P., Akaho, E. H. K., Nyarko, B. J. B., and Yamoah, S., 2012, "Modeling and Simulation of Cogeneration Nuclear Power Plant for Seawater Desalination," Nucl. Eng. Des., **242**(1), pp. 143–147.

[9] Yan, X., Yan, X., Tachibana, Y., Ohashi, H., Sato, H., Tazawa, Y., and Kunitomi, K., 2013, "A Small Modular Reactor Design for Multiple Energy Applications: HTR50S," Nucl. Eng. Technol., **45**(3), pp. 401–414.

[10] AlZahrani, A. A., and Dincer, I., 2015, "Performance Assessment of an Aquifer Thermal Energy Storage System for Heating and Cooling Applications," ASME J. Energy Res. Technol., **138**(1), p. 011901.

[11] Homan, K. O., 2003, "Internal Entropy Generation Limits for Direct Sensible Thermal Storage," ASME J. Energy Res. Technol., **125**(2), pp. 85–93.

[12] Derakhshan, S., and Khosravian, M., 2019, "Exergy Optimization of a Novel Combination of a Liquid Air Energy Storage System and a Parabolic Trough Solar Collector Power Plant," ASME J. Energy Res. Technol., **141**(8), p. 081901.

[13] Jalalzadeh-Azar, A. A., 1996, "Heat Transfer in a High-Temperature Packed Bed Thermal Energy Storage System—Roles of Radiation and Intraparticle Conduction," ASME J. Energy Res. Technol., **118**(1), pp. 50–57.

[14] Benato, A., 2018, "Energy and Cost Analysis of a New Packed Bed Pumped Thermal Electricity Storage Unit," ASME J. Energy Res. Technol., **140**(2), p. 020904.

[15] Allen, K. G., Backström, T. W., and Kröger, D. G., 2014, "Packed Rock Bed Thermal Storage in Power Plants: Design Considerations," Energy Procedia, **49**(1), pp. 666–675.

[16] Waked, A. M., 1986, "Solar Energy Storage in Rocks," Solar Wind Technol., **3**(1), pp. 27–31.

[17] Reuss, M., 2015, "6—The Use of Borehole Thermal Energy Storage (BTES) Systems," *Advances in Thermal Energy Storage Systems* (Woodhead Publishing Series in Energy), L. F. Cabeza, ed., Woodhead Publishing, Sawston, Cambridge, pp. 117–147.

[18] Frick, K., Misenheimer, C. T., Doster, J. M., Terry, S. D., and Bragg-Sitton, S., 2018, "Thermal Energy Storage Configurations for Small Modular Reactor Load Shedding," Nucl. Technol., **202**(1), pp. 53–70.

[19] Alameri, S., 2015, *A Coupled Nuclear Reactor Thermal Energy Storage System for Enhanced Load Following Operation*, Colorado School of Mines, Golden, Colorado.

[20] Sabharwall, P., Green, M., Yoon, S., Bragg-Sitton, S., and Stoots, C., 2014, "Nuclear Hybrid Energy Systems: Molten Salt Energy Storage," No. INL/CON-13-30025. Idaho National Laboratory (INL), Technical Report.

[21] Mollenhauer, E., Christidis, A., and Tsatsaronis, G., 2018, "Increasing the Flexibility of Combined Heat and Power Plants With Heat Pumps and Thermal Energy Storage," ASME J. Energy Res. Technol., **140**(2), p. 020907.

[22] Caputo, A. C., Palumbo, M., Pelagagge, P. M., and Scacchia, F., 2005, "Economics of Biomass Energy Utilization in Combustion and Gasification Plants: Effects of Logistic Variables," Biomass Bioenergy, **28**(1), pp. 35–51.

[23] Pacheco, J. E., Showalter, S. K., and Kolb, W. J., 2002, "Development of a Molten-Salt Thermocline Thermal Storage System for Parabolic Trough Plants," ASME J. Sol. Energy Eng., **124**(2), pp. 153–159.

[24] Eastman, 2006, "Therminol-VP1 Heat Transfer Fluid," Technical Report of the Fluid Properties. https://www.therminol.com/sites/therminol/files/documents/TF09A_Therminol_VP1.pdf